

## Automated Vickers hardness system with closed-loop control for polishing pads for semiconductor production

Le Nam Quoc Huy, Le Ngoc Quynh Hoa, Muhamad Amirul Haq & Tan-Thanh Huynh

**To cite this article:** Le Nam Quoc Huy, Le Ngoc Quynh Hoa, Muhamad Amirul Haq & Tan-Thanh Huynh (16 Nov 2023): Automated Vickers hardness system with closed-loop control for polishing pads for semiconductor production, Instrumentation Science & Technology, DOI: [10.1080/10739149.2023.2281538](https://doi.org/10.1080/10739149.2023.2281538)

**To link to this article:** <https://doi.org/10.1080/10739149.2023.2281538>



Published online: 16 Nov 2023.



Submit your article to this journal [↗](#)



View related articles [↗](#)



View Crossmark data [↗](#)



# Automated Vickers hardness system with closed-loop control for polishing pads for semiconductor production

Le Nam Quoc Huy<sup>a</sup> , Le Ngoc Quynh Hoa<sup>b</sup> , Muhamad Amirul Haq<sup>c</sup> ,  
and Tan-Thanh Huynh<sup>d</sup> 

<sup>a</sup>Department of Mechanical Engineering, National Taiwan University of Science and Technology, Taipei, Taiwan; <sup>b</sup>Emerging Nanoscience Research Institute (EnRI), Nanyang Technological University, Singapore; <sup>c</sup>Department of Electronic and Computer Engineering, National Taiwan University of Science and Technology, Taiwan; <sup>d</sup>School of Applied Chemistry, Tra Vinh University, Vietnam

## ABSTRACT

Chemical mechanical polishing plays a pivotal role in enhancing the topography of wafers during semiconductor fabrication. The hardness of polishing pads holds great significance as it determines the material removal rate during the planarization process. Hence, precise determination of polishing pad hardness at both micro and macro scales is essential for optimizing the semiconductor polishing process, ensuring the prevention of wafer erosion or dishing. In this study, an automated system was developed for determining Vickers hardness of microporous polishing pads employing a closed-loop control method. The system was calibrated based on the relationship between load-unloading force and displacement observed in Vickers indentation experiments. The designed apparatus is not only successfully verified with standard values for Vickers reference blocks with less than 2% error, but it also demonstrated a smaller average relative error percentage than the commercial system using traditional open-loop measurement method. The closed-loop Vickers hardness apparatus proves to be a promising alternative for measuring hardness accurately, particularly in samples with noisy surfaces, rough surfaces, and porous microstructures.

## KEYWORDS

Vickers hardness testing; closed-loop control technology; force-displacement response; polishing pad hardness; semiconductor fabrication

## Introduction

The hardness measurement is widely used in the field of material testing and research due to its simplicity, affordability, and reliability of evaluating properties without the use of destructive methods. These tests involve pressing a small indenter tip onto the surface of testing specimens with a specific force, allowing for analysis of the resulting surface deformations.<sup>[1–</sup>

**CONTACT** Tan-Thanh Huynh  [htthan@tvu.edu.vn](mailto:htthan@tvu.edu.vn)  School of Applied Chemistry, Tra Vinh University, Vietnam.

<sup>4]</sup> Among the various indenter shapes available, such as pyramids with square, triangular, or rhomboid bases, the Vickers hardness technique is discussed in this study. Vickers hardness is a popular method due to its experimental simplicity and applicability to all types of materials.<sup>[5–8]</sup>

In traditional open-loop method, human operators rely on visual observation of indentation marks using images captured by a camera connected to a microscope. However, accurately detecting and analyzing these marks can be challenging due to variations in material properties, potential contamination, surface defects resulting from mechanical treatment, and the expertise and working conditions of the operators.<sup>[9,10]</sup> To address these challenges, computer systems utilizing digital image processing and data analysis have been developed to identify the diagonal lengths of indentation marks. Nevertheless, these methods encounter difficulties caused by variations in illumination conditions, changes in image appearance due to different indenter loads or the material with a transparent surface, such as polymers or porous materials, and the need to polish the material's surface before hardness testing, leading to discrepancies between the actual and experimental surface conditions.<sup>[11–13]</sup> To overcome these limitations and optimize the automation of equipment in different environments while reducing human involvement, in this study, the development of a closed-loop Vickers hardness apparatus is reported. The theoretical framework of the closed-loop apparatus is based on the Oliver-Pharr model, which establishes a relationship between force and displacement of the Vickers pyramidal indenter diamond tip during hardness indentation experiments to determine the projected contact area between testing sample and indenter tip, allowing for accurate calibration.<sup>[14–19]</sup>

The designed apparatus underwent meticulous validation by comparing the relative error from Vickers indentation experiments with those of reference blocks. There is remarkable agreement between the closed-loop control method developed for the Vickers hardness apparatus and testing machine with traditional open-loop control method based on mean relative percentage with errors as low as 2%.

The applicability of the apparatus was demonstrated by measuring the Vickers hardness of a microporous structure polishing pad (IC1000, Dow Chemical, Michigan, USA), commonly utilized in semiconductor manufacturing processes.<sup>[20–23]</sup> The obtained hardness results were compared to those obtained using the traditional open-loop method Vickers hardness instrument, further highlighting the precision of the designed system. Therefore, the design and verification approach can serve as a new reference for the development of Vickers hardness instrumentation. Moreover, when considering the relationship between loading and displacement during indentation, experiments can result in an optimized bulk material

structure. The designed apparatus system also permits the use of other types of indentation tips, such as cone tip and Knoop indenter tip, as well as the designed 3-side indenter tips *via* the movement arm.

## The design of Vickers hardness testing apparatus

### Theoretical aspects

In this study, the employment of closed-loop control technology enables the continuous assessment and regulation of the indentation force exerted on the sample surface. This is accomplished with the designed Vickers hardness apparatus. The Vickers hardness of the material is determined based on the load-displacement data gathered during the process of loading and unloading the axisymmetric indenter diamond tip. This process is graphically represented in Figure 1.

The hardness of material is described as the proportion of the normal force exerted on an indentation tip to the projected contact area. To ascertain the true contact area, Oliver and Pharr suggested that it could be established by examining the contact depth ( $h_c$ ) during indentation experiments.<sup>[24–27]</sup> This contact depth can be calibrated using the maximum

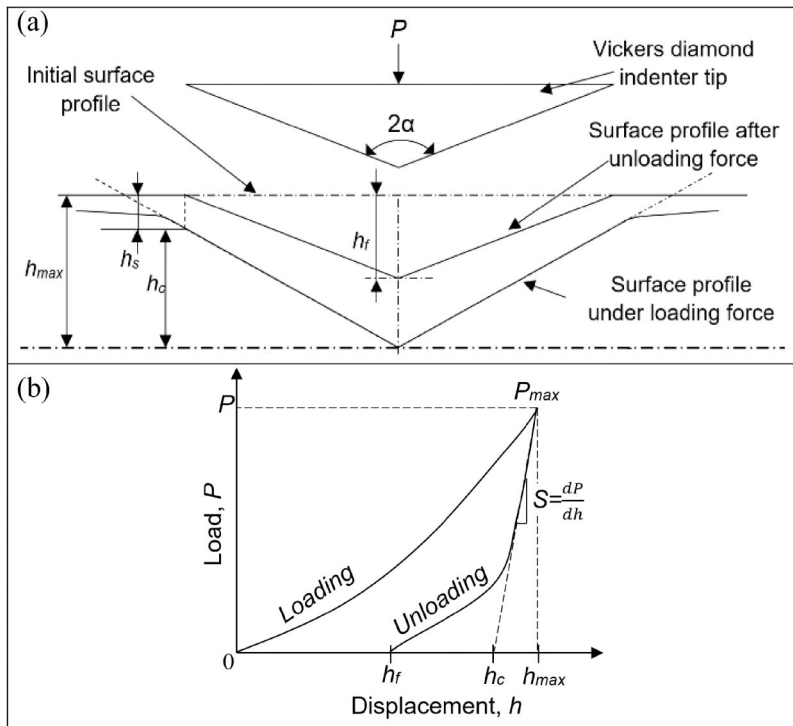


**Figure 1.** (a) Main profile parameters of the surface material before and after Vickers indentation measurement. (b) Schematic of load  $P$  and depth  $h$  for an indentation experiment.

indentation depth ( $h_{max}$ ) and the depth of deflection ( $h_f$ ) at the highest load ( $P_{max}$ ). The equation for contact depth in an indentation experiment is described by:

$$h_c = h_{max} - \varepsilon \frac{P_{max}}{dP/dh} \quad (1)$$

where  $\varepsilon$  is a constant which relies on the geometry of the Vickers diamond indenter tip and is typically around 0.75 for a Vickers diamond tip.<sup>[28–31]</sup> The contact area is then calculated based on the geometrical relationship of the indenter's half-angle for a Vickers pyramidal diamond indenter tip as shown by

$$h_c = \frac{\sqrt{A_c}}{2 \tan \alpha} \quad (2)$$

where  $\alpha$  represents the half angle of the Vickers indenter, 68 degrees. Once the contact area ( $A_c$ ) is determined, the Vickers hardness of a material based on closed-loop control technology ( $HV_c$ ) can be determined by using its standard definition:<sup>[32–34]</sup>

$$HV_c = \frac{P_{max}}{A_c} \quad (3)$$

### **Description of the Vickers hardness apparatus**

As part of this study, the designed Vickers hardness apparatus is used to characterize the material. This is accomplished through a closed-loop feedback control system equipped with a Vickers diamond tip. The schematic layout of this instrument is presented in [Figure 2](#). The instrument comprises a high-precision linear positioning stage responsible for the vertical motion of the Vickers indenter holder. This vertical motion is driven by a deceleration DC gear motor (JGY-370, Aslong, Shenzhen, China), with a height travel range varying from 0 to 10 mm. The deceleration DC motor features a special reduction gear structure that ensures the main unit shaft is securely locked during idle periods to maintain load balance. A jaw coupling is employed to establish a connection between the shaft of the deceleration motor and the screw of the high-precision linear positioning stage, driving the linear movement arm.

To calibrate the vertical movement of the elevation stage during the motor's rotation, a high-accuracy magnetic rotary encoder (MES 2500, Fotek, Taipei, Taiwan) is integrated into another shaft of the deceleration motor. This encoder measures the crank angle position with a resolution of 2500 pulses per revolution (PPR). The S-type load cell (2 kg, HT sensors technology Co LTD, Xi-an, China) is installed at the rear of the diamond

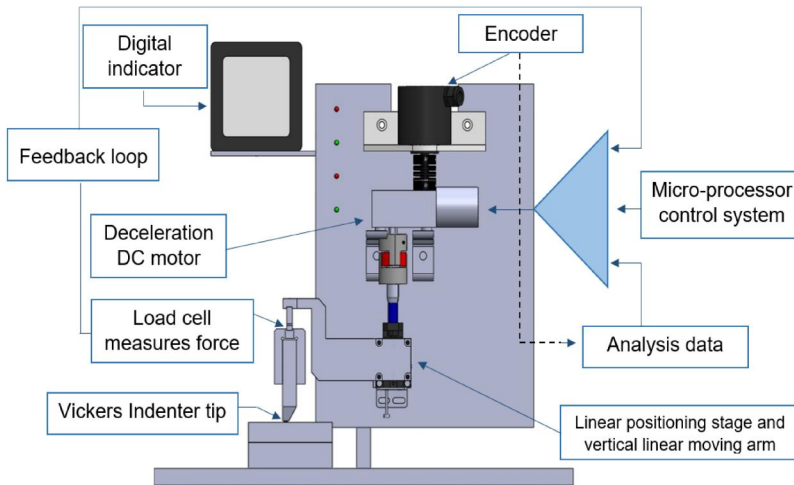


**Figure 2.** Schematic of the designed Vickers hardness testing apparatus.

indenter tip holder and the vertical linear moving arm, facilitating the analysis of the normal force during Vickers indentation tests. Furthermore, the instrument's control system employs a NI USB-6351 X-Series DAQ device (National Instruments, Austin, TX, USA) and LabVIEW 2020 programming (National Instruments, Austin, TX, USA) to control the system. The light emitting diodes (LEDs) signify the indentation procedure's progress, while a digital lock displays the real-time loading force value during the indentation process.

## Results and discussion

### *Vickers hardness determination by using traditional method*

In this experimental investigation, a range of commercial Vickers hardness standard blocks was employed obtained from Mitutoyo (Tokyo, Japan), with hardness values spanning from 500 HV0.05 to 500 HV1. The aim of the study was to conduct Vickers hardness tests using two distinct methodologies: the traditional open-loop method utilizing a commercial Vickers hardness instrument (Matsuzawa DVK-1S, Akashi, Japan), and a novel approach employing the designed apparatus, which incorporated a closed-loop feedback system.

The Vickers hardness indentation testing procedure was conducted on the standard blocks, utilizing indent loads ranging from 50 gf to 1000 gf, with a constant dwelling time of 10 s at room temperature. Additionally, the indentation rate was set at 0.2 mm/min, and the loading time was controlled based on the maximum load applied. In order to determine the average Vickers hardness values for each specific loading value, a total of five indentations were performed for each. The mean Vickers hardness

obtained through the traditional open-loop method ( $HV_o$ ) was calculated by.<sup>[35–38]</sup>

$$HV_o = 1.854 \frac{F}{d^2} \quad (4)$$

where  $F$  is the applied load (measured in kilograms-force) and  $d$  is the average diagonal length of the indentation (measured in millimeter). The comparison between open-loop hardness measurement and standard Vickers hardness values from standard blocks was performed using the relative error ( $RE\%$ ):

$$RE\% = \left| \frac{S_i - \bar{M}_i}{S_i} \right| \times 100 \quad (5)$$

where  $S_i$  and  $\bar{M}_i$  are Vickers hardness standard and average Vickers hardness values from experiments. The sizes of the indentation marks are determined using a scanning electron microscope (SEM). According to the results of Vickers indentation on standard test blocks, the average relative error percentages have decreased significantly from 1.86% at 500 HV0.05 to 0.72% at 500 HV0.3. Conversely, with an increase in the loading force from 300 gf to 1000 gf, the average relative error exhibited a slight decline, averaging at approximately 0.35%. Notably, the large fluctuations in the average relative error observed at low loading forces can be attributed to the small size of the indentation marks, which significantly influences the determination of the diagonal length.

### ***Vickers hardness designed apparatus validation and application***

The apparatus utilized a Vickers diamond indenter tip with a 136 degrees opening angle, manufactured by Charming, Shanghai Diamond Industry. The primary objective of the verification tests was to evaluate the accuracy of the closed-loop control method implemented in the designed Vickers hardness apparatus when compared to the open-loop commercial instrument. The results obtained from the open-loop testing provided the basis for validating the closed-loop apparatus. Additionally, the closed-loop apparatus used the theoretical framework described above to calibrate the Vickers hardness. The indentation experiments were carried out with precise force control using a system designed with LabVIEW software.

The analysis of the loading-unloading force values and displacement curves during the indentation experiment of the Vickers diamond tip consisted of three steps. Initially, in Step 1, the indenter was driven by a deceleration DC motor until it made contact with the surface of the testing specimen, and the initial position was detected by a force sensor. Subsequently, in Step 2, an application-designed system based on LabVIEW

software controlled the applied force and dwell time. The deceleration DC motor drove the Vickers diamond indenter tip to achieve the desired force setup, while an encoder calibrated the indentation depth during the loading process. Finally, in Step 3, the diamond indenter tip retreated from the specimen, returning to its initial position, and the final indentation depth was defined as the depth of the material's surface after unloading the force.

The closed-loop control method for Vickers hardness testing was applied to the same Vickers hardness standard blocks as well as the same experimental conditions for the traditional open-loop method. To calibrate the Vickers hardness values based on the theoretical principles, a mathscript was developed and integrated into a LabVIEW application. This enabled the comprehensive analysis of Vickers hardness, with a specific focus on the relationship between load-unloading force and displacement during indentation tests.

The results of the Vickers hardness standard blocks under indentation tests are summarized and visually presented in [Figure 3\(a\)](#). Moreover, to capture the detailed three-dimensional (3D) geometry of the residual imprints left by the Vickers indentation marks after unloading, high-definition laser confocal microscopy LEXT OLS5100 (Olympus, Tokyo, Japan) with a 50x objective lens was employed, as depicted in [Figure 3\(b\)](#).

It is noteworthy that the closed-loop Vickers hardness apparatus-designed system demonstrated remarkable accuracy in determining the final depth of the indentation marks, as the obtained measurements exhibited strong correlation with the results obtained from laser confocal scanning examinations.

The testing results of Vickers hardness on standard blocks obtained using two methods, as illustrated in [Figure 4](#), clearly demonstrate a consistent trend of decreasing average relative error as the loading force increases from 50 gf to 1000 gf. Notably, there is a considerable variation in the average relative error of open-loop method (OP) and closed-loop (CP) based on indentation loads between 50 gf and 100 gf. The increase in the average relative error in the open-loop method can be attributed to the inherent challenges associated with accurately determining the diagonal lengths of indentation marks using optical measurements, particularly when dealing with small indentation marks at low loading forces. In contrast, the closed-loop method effectively addresses this challenge by calibrating the force-displacement relationship during the indentation experiments, providing a comprehensive solution. Consequently, the average relative error of closed-method largely depends on the surface roughness of Vickers hardness reference blocks at low loading forces. Conversely, when the loading forces range from 200 gf to 1000 gf, the difference in relative error between the two methods is relatively small. This can be attributed to the increased

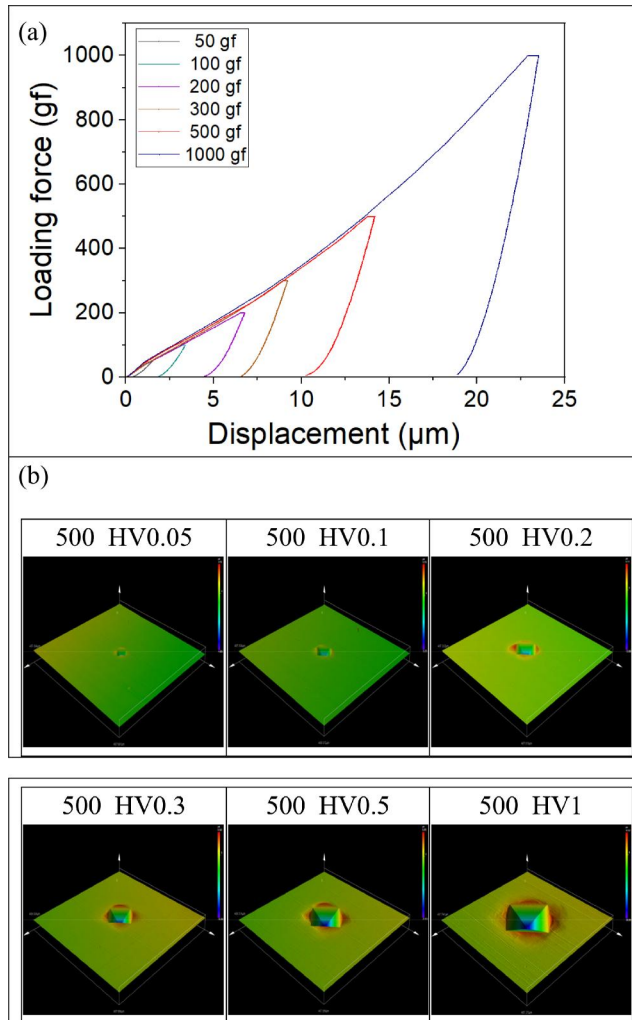


**Figure 3.** (a) Analyzing load-displacement curves of Vickers standard blocks using the closed-loop indentation method. (b) Analyzing the final indentation depth with confocal laser scanning.

ease of determining the exact length of an indentation mark through the open-loop measurement. Furthermore, the surface roughness of the Vickers hardness reference blocks does not appear to be significantly affected by the closed-loop approach.

In comparison to an open-loop Vickers hardness system, the designed closed-loop apparatus exhibits lower average relative error, with an average error of less than 2% when tested with reference blocks. This highlights the suitability of the designed apparatus for accurate hardness measurements of various materials.

As part of this study, the designed apparatus was employed to determine the hardness of microporous polishing pad IC1000 utilized in polishing for

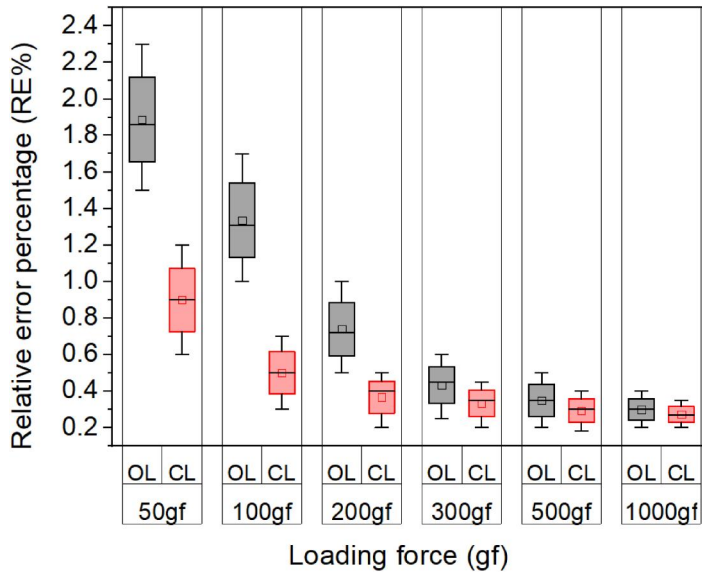


**Figure 4.** Comparison of average relative error between two methods of Vickers hardness measurement using reference blocks.

semi-conductor fabrication. A loading force ranging from 100 gf to 500 gf is applied to the microporous polishing pad IC1000 to assess its hardness, corresponding to the employed diamond dressing pad process.

The Vickers indentation test was conducted in triplicate for each maximum control loading force on the microporous polishing pad IC1000. [Figure 5\(a\)](#) showcases the relationship between the loading-unloading force and displacement observed during Vickers indentation of the microporous polishing pad IC1000 using the closed-loop designed system. Additionally, the hardness results obtained from the closed-loop apparatus were cross-validated with the traditional open-loop system. [Figure 5\(b\)](#) presents a comprehensive comparison between the hardness values of the microporous polishing pad IC1000 obtained through both methods and the resulting indentation marks on the pad's surface. The determination of the diagonal length of indentation marks was achieved through image processing of laser scanning confocal images, which served as a calibration method for Vickers hardness in the open-loop approach. With an increase in loading force from 100 gf to 300 gf, the average Vickers hardness value of the microporous polishing pad IC1000 exhibited a significant decline, ranging from 42.2 HV to 39.9 HV. However, when the loading force was further increased from 300 gf to 500 gf, the Vickers hardness of the microporous polishing pad IC1000 remained relatively constant, averaging at 39.2 HV. The designed apparatus, capable of adjusting the loading force, enables comprehensive assessment of material hardness from micro to macro scales, making it suitable for diverse applications. Furthermore, the verification

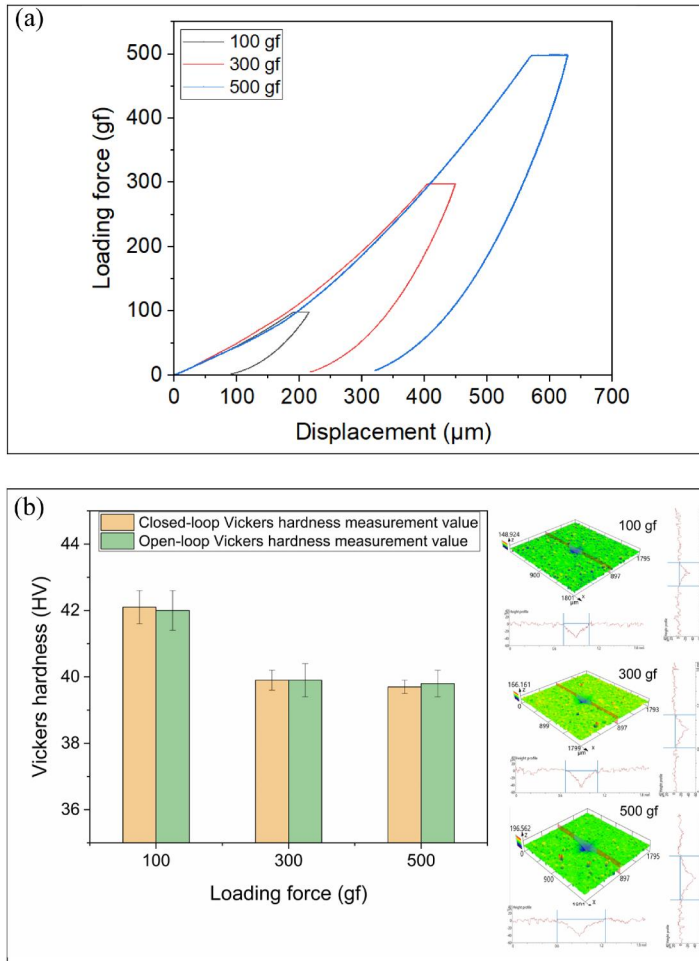


**Figure 5.** (a) Analysis of the load-unloading force and displacement curves of Vickers indentation for the microporous structure polishing pad IC1000 using a closed-loop system; (b) Comparison of the Vickers hardness and the analysis of diagonal length of Vickers indentation marks on the IC1000 polishing pad's surface.

demonstrated a close agreement between the calibrations obtained by the closed-loop system and the results obtained by the open-loop system, with a difference of less than 3% in average values between the two methods. Discrepancies in Vickers hardness values between the two approaches can be attributed to the determination of diagonal lengths of indentation marks, which relies on image analysis in the open-loop procedure.

## Conclusions

In this paper, we proposed an innovative approach to the closed-loop Vickers hardness apparatus offers advantages over traditional open-loop methods. By operating under variable loading conditions and mitigating

challenges related to visual inspection and human influence, the proposed approach provides enhanced accuracy and reliability. The calibration of the designed apparatus, based on load-displacement curves, has been rigorously validated by comparing the average relative error percentages with Vickers hardness values of reference test blocks, resulting in an error rate of less than 2%. Furthermore, the Vickers hardness of the microporous structure polishing pad IC1000 was successfully determined using the designed closed-loop apparatus. To ensure the validity of the results, the measurements were cross-validated using the traditional open-loop measurements. This demonstrates the effectiveness and versatility of the designed apparatus in accurately determining hardness values for materials with diverse structures and surfaces. This approach holds significant potential for calculating the material removal rate in semiconductor manufacturing, particularly in chemical mechanical polishing of wafers. By providing precise hardness measurements of polishing pads, it enables better control and optimization of the planarization procedure, ultimately enhancing the quality and efficiency of semiconductor fabrication.

### Disclosure statement

There are no known competing financial interests or personal relationships that influenced the work reported in this article.

### ORCID

Le Nam Quoc Huy  <http://orcid.org/0000-0002-2015-4272>

Le Ngoc Quynh Hoa  <http://orcid.org/0000-0002-2515-3463>

Muhamad Amirul Haq  <http://orcid.org/0000-0003-1516-0229>

Tan-Thanh Huynh  <http://orcid.org/0000-0002-6097-2528>

### References

- [1] Anthony Xavier, M.; Manohar, M.; Madhukar, P. M.; Jeyapandiarajan, P. Experimental Investigation of Work Hardening, Residual Stress and Microstructure during Machining Inconel 718. *J. Mech. Sci. Technol.* **2017**, *31*, 4789–4794. DOI: [10.1016/j.matpr.2018.02.322](https://doi.org/10.1016/j.matpr.2018.02.322).
- [2] Leu, D. K. Evaluation of Friction Coefficient Using Indentation Model of Brinell Hardness Test for Sheet Metal Forming. *J. Mech. Sci. Technol.* **2011**, *25*, 1509–1517. DOI: [10.1007/s12206-011-0134-4](https://doi.org/10.1007/s12206-011-0134-4).
- [3] Li, L.; Khraishi, T.; Shen, Y.-L. Investigation of the Effect of Indentation Spacing, Edge Distance and Specimen Thickness on the Measurement of Hardness. *J. Mech. Sci. Technol.* **2023**, *37*, 687–696. DOI: [10.1007/s12206-023-0112-7](https://doi.org/10.1007/s12206-023-0112-7).
- [4] Huy, L. N. Q.; Hoa, L. N. Q.; Chen, C.-C. A. **2022** Study on Force Analysis for Elastomer Pad by Single Diamond Tool. In International Conference on

- Planarization Technology, Portland, the United States. <https://hal.science/hal-04084340/>.
- [5] Shahdad, S. A.; McCabe, J. F.; Bull, S.; Rusby, S.; Wassell, R. W. Hardness Measured with Traditional Vickers and Martens Hardness Methods. *Dent. Mater.* **2007**, *23*, 1079–1085. DOI: [10.1016/j.dental.2006.10.001](https://doi.org/10.1016/j.dental.2006.10.001).
- [6] Yehia, H. M.; Abdelalim, N.; El-Mahallawi, I.; Abd-Elmotaleb, T.; Hoziefa, W. Characterization of Swarf Al/(Al<sub>2</sub>O<sub>3</sub>/GNs) Ag Composite Fabricated Using Stir Casting and Rolling Process. *J. Mech. Sci. Technol.* **2023**, *37*, 1803–1809. DOI: [10.1007/s12206-023-0320-1](https://doi.org/10.1007/s12206-023-0320-1).
- [7] Schneider, J.-M.; Bigerelle, M.; Iost, A. Statistical Analysis of the Vickers Hardness. *Mater. Sci. Eng. A.* **1999**, *262*, 256–263. DOI: [10.1016/S0921-5093\(98\)01000-4](https://doi.org/10.1016/S0921-5093(98)01000-4).
- [8] Huy, L. N. Q.; Lin, C.-Y.; Chen, C.-C. A Study on Evaluation Hardness of Porous Pad for Chemical Mechanical Polishing. In *38th National Academic Symposium (CSME2021)*, Tainan, Taiwan, **2021**. <https://hal.science/hal-04080545/>.
- [9] Ghorbani, S.; Hoseinie, S. H.; Ghasemi, E.; Sherizadeh, T. A Review on Rock Hardness Testing Methods and Their Applications in Rock Engineering. *Arab. J. Geosci.* **2022**, *15*, 1067. DOI: [10.1007/s12517-022-10314-z](https://doi.org/10.1007/s12517-022-10314-z).
- [10] Soni, V. K.; Sinha, A. K. Effect of Alloying Elements, Phases and Heat Treatments on Properties of High-Entropy Alloys: A Review. *Trans. Indian Inst. Met.* **2023**, *76*, 897–914. DOI: [10.1007/s12666-022-02777-1](https://doi.org/10.1007/s12666-022-02777-1).
- [11] Li, Z.; Yin, F. Automated Measurement of Vickers Hardness Using Image Segmentation with Neural Networks. *Meas. Sci. Technol.* **2021**, *186*, 110200. DOI: [10.1016/j.measurement.2021.110200](https://doi.org/10.1016/j.measurement.2021.110200).
- [12] Dominguez-Nicolas, S. M.; Wiederhold, P. **2018** Indentation Image Analysis for Vickers Hardness Testing. In *International Conference on Electrical Engineering, Computing Science and Automatic Control (CCE)*; Mexico City, Mexico; pp. 1–6.
- [13] Khatavkar, N.; Swetlana, S.; Singh, A. K. Accelerated Prediction of Vickers Hardness of Co-and Ni-Based Superalloys from Microstructure and Composition Using Advanced Image Processing Techniques and Machine Learning. *Acta Mater.* **2020**, *196*, 295–303. DOI: [10.1016/j.actamat.2020.06.042](https://doi.org/10.1016/j.actamat.2020.06.042).
- [14] Nazemian, M.; Chamani, M. Experimental Investigation and Finite Element Simulation of the Effect of Surface Roughness on Nanoscratch Testing. *J. Mech. Sci. Technol.* **2019**, *33*, 2331–2338. DOI: [10.1007/s12206-019-0432-9](https://doi.org/10.1007/s12206-019-0432-9).
- [15] Huy, L. N. Q.; Lin, C.-Y.; Chen, C.-C. A. Analyzing the Effects of Pad Asperity on Chemical Mechanical Polishing of Copper Thin Film Wafer. *Jpn. J. Appl. Phys.* **2022**, *61*, 071005. DOI: [10.35848/1347-4065/ac78b2](https://doi.org/10.35848/1347-4065/ac78b2).
- [16] Dar, U. A.; Zhang, W. Polymer Based Aerospace Structures under High Velocity Impact Applications; Experimental, Constitutive and Finite Element Analysis. *J. Mech. Sci. Technol.* **2015**, *29*, 4259–4265. DOI: [10.1007/s12206-015-0922-3](https://doi.org/10.1007/s12206-015-0922-3).
- [17] Rao, X.; Zhang, F.; Luo, X.; Ding, F. Characterization of Hardness, Elastic Modulus and Fracture Toughness of RB-SiC Ceramics at Elevated Temperature by Vickers Test. *Mater. Sci. Eng. A.* **2019**, *744*, 426–435. DOI: [10.1016/j.msea.2018.12.044](https://doi.org/10.1016/j.msea.2018.12.044).
- [18] Lim, Y. Y.; Chaudhri, M. M. Indentation of Elastic Solids with a Rigid Vickers Pyramidal Indenter. *Mech. Mater.* **2006**, *38*, 1213–1228. DOI: [10.1016/j.mechmat.2006.04.006](https://doi.org/10.1016/j.mechmat.2006.04.006).
- [19] Huy, L. N. Q.; Hoa, L. N. Q.; Chen, C.-C. A. Modeling of Material Removal in Copper Blanket Wafer Polishing Based on the Hard Polishing Pad Microstructure. *Int. J. Adv. Manuf. Technol.* **2023**, *128*, 4455–4468. DOI: [10.1007/s00170-023-12204-4](https://doi.org/10.1007/s00170-023-12204-4).

- [20] Lu, H.; Obeng, Y.; Richardson, K. A. Applicability of Dynamic Mechanical Analysis for CMP Polyurethane Pad Studies. *Mater. Charact.* **2002**, *49*, 177–186. DOI: [10.1016/S1044-5803\(03\)00004-4](https://doi.org/10.1016/S1044-5803(03)00004-4).
- [21] Rogers, C.; Coppeta, J.; Racz, L.; Philipossian, A.; Kaufman, F. B.; Bramono, D. Analysis of Flow between a Wafer and Pad during CMP Processes. *J. Elec. Materi.* **1998**, *27*, 1082–1087. DOI: [10.1007/s11664-998-0141-0](https://doi.org/10.1007/s11664-998-0141-0).
- [22] Castillo-Mejia, D.; Gold, S.; Burrows, V.; Beaudoin, S. The Effect of Interactions between Water and Polishing Pads on Chemical Mechanical Polishing Removal Rates. *J. Electrochem. Soc.* **2003**, *150*, G76–G82. DOI: [10.1149/1.1531973](https://doi.org/10.1149/1.1531973).
- [23] Kim, B.S.; Tucker, M.H.; Kelchner, J.D.; Beaudoin, S.P. Study on the Mechanical Properties of CMP Pads. *IEEE Trans. Semicond. Manufact.* **2008**, *21*(3), 454–463. DOI: [10.1109/TSM.2008.2001223](https://doi.org/10.1109/TSM.2008.2001223).
- [24] Oliver, W. C.; Pharr, G. M. An Improved Technique for Determining Hardness and Elastic Modulus Using Load and Displacement Sensing Indentation Experiments. *J. Mater. Res.* **1992**, *7*, 1564–1583. DOI: [10.1557/JMR.1992.1564](https://doi.org/10.1557/JMR.1992.1564).
- [25] Pharr, G. M.; Bolshakov, A. Understanding Nanoindentation Unloading Curves. *J. Mater. Res.* **2002**, *17*, 2660–2671. DOI: [10.1557/JMR.2002.0386](https://doi.org/10.1557/JMR.2002.0386).
- [26] Hay, J. C.; Bolshakov, A.; Pharr, G. M. A Critical Examination of the Fundamental Relations Used in the Analysis of Nanoindentation Data. *J. Mater. Res.* **1999**, *14*, 2296–2305. DOI: [10.1557/JMR.1999.0306](https://doi.org/10.1557/JMR.1999.0306).
- [27] Huy, L. N. Q.; Hoa, L. N. Q. **2023** A Study on Force Analysis of Single Diamond Tools for Elastomer Polishing Pads Used in the Diamond Dressing Process. In *International Conference on Precision Engineering and Sustainable Manufacturing (PRESM2023)*, Okinawa, Japan. <https://hal.science/hal-04158220/>.
- [28] Huy, L. N. Q.; Hoa, L. N. Q. An Investigation of the Vickers Hardness of Polishing Pads Using Simulations Based on Microtomography Model. *Jpn. J. Appl. Phys.* **2023**, *62*, 056502. DOI: [10.35848/1347-4065/acd42a](https://doi.org/10.35848/1347-4065/acd42a).
- [29] Oliver, W. C.; Pharr, G. M. Measurement of Hardness and Elastic Modulus by Instrumented Indentation: Advances in Understanding and Refinements to Methodology. *J. Mater. Res.* **2004**, *19*, 3–20. DOI: [10.1557/jmr.2004.19.1.3](https://doi.org/10.1557/jmr.2004.19.1.3).
- [30] Fang, T.-H.; Chang, W.-Y.; Huang, J.-J. Dynamic Characteristics of Nanoindentation Using Atomistic Simulation. *Acta. Mater.* **2009**, *57*, 3341–3348. DOI: [10.1016/j.actamat.2009.03.048](https://doi.org/10.1016/j.actamat.2009.03.048).
- [31] Huy, L. N. Q.; Lin, C.-Y.; Chen, C.-C. A. Development of Modeling to Investigate Polyurethane Pad Hardness in Chemical Mechanical Planarization/Polishing (CMP) Process. *Jpn. J. Appl. Phys.* **2022**, *61*, SJ1002. DOI: [10.35848/1347-4065/ac6a3a](https://doi.org/10.35848/1347-4065/ac6a3a).
- [32] Alamgir, M.; Mallick, A.; Nayak, G. C.; Tiwari, S. K. Development of PMMA/TiO<sub>2</sub> Nanocomposites as Excellent Dental Materials. *J. Mech. Sci. Technol.* **2019**, *33*, 4755–4760. DOI: [10.1007/s12206-019-0916-7](https://doi.org/10.1007/s12206-019-0916-7).
- [33] Sakharova, N. A.; Fernandes, J. V.; Antunes, J. M.; Oliveira, M. C. Comparison between Berkovich, Vickers and Conical Indentation Tests: A Three-Dimensional Numerical Simulation Study. *Int. J. Solids Struct.* **2009**, *46*, 1095–1104. DOI: [10.1016/j.ijsolstr.2008.10.032](https://doi.org/10.1016/j.ijsolstr.2008.10.032).
- [34] Nguyen, N.-V.; Kim, S.-E. Experimental Study to Investigate Microstructure and Continuous Strain Rate Sensitivity of Structural Steel Weld Zone Using Nanoindentation. *Int. J. Mech. Sci.* **2020**, *174*, 105482. DOI: [10.1016/j.ijmecsci.2020.105482](https://doi.org/10.1016/j.ijmecsci.2020.105482).
- [35] American Society of Testing Materials: ASTM C373-18. West Conshohocken, PA: ASTM International. 1994.

- [36] Safarzadeh, M.; Chee, C. F.; Ramesh, S. Effect of Carbonate Content on the *In Vitro* Bioactivity of Carbonated Hydroxyapatite. *Ceram. Int.* **2022**, *48*, 18174–18179. DOI: [10.1016/j.ceramint.2022.03.076](https://doi.org/10.1016/j.ceramint.2022.03.076).
- [37] Lin, M.; Jiang, D.; Li, L.; Lu, Z.; Lai, T.; Shi, J. The Effect of Creep Deformation of a  $\beta$  Sialon on Vickers Hardness, Fracture Toughness and Weibull Modulus. *Mater. Sci. Eng. A.* **2003**, *351*, 9–14. DOI: [10.1016/S0921-5093\(01\)01772-5](https://doi.org/10.1016/S0921-5093(01)01772-5).
- [38] Huy, L. N. Q.; Chen, C.-C. A. Effects of Grits Size on Diamond Wire Sawing Process of Monocrystalline Silicon Wafers. In *International Symposium on Precision Engineering and Sustainable Manufacturing (PRESM2021)*, Jeju, Korea, **2021**. <https://hal.science/hal-04015508/>.